2162-8769/2013/2(7)/P293/6/$31.00 © The Electrochemical Society

Microwave Annealing of Phosphorus and Cluster Carbon Implanted (100) and (110) Si

Ta-Chun Cho,[a] Yu-Lun Lu,[a] Jie-Yi Yao,[b] Yao-Jen Lee,[b,z] Karuppanan Sekar,[c,d] Nobuhiro Tokoro,[c,d] Hiroshi Onoda,[e] Wade Krull,[d] Michael I. Current,[f] and Tien-Sheng Chao[a]

[a]*Department of Electrophysics, National Chiao Tung University, Hsinchu 300, Taiwan*
[b]*National Nano Device Laboratories, Hsinchu 300, Taiwan*
[c]*Nissin Ion Equipment USA Inc, North Billerica, Massachusetts 01862, USA*
[d]*SemEquip Inc, North Billerica, Massachusetts 01862, USA*
[e]*Nissin Ion Equipment Co. Ltd, Kyoto 601-8205, Japan*
[f]*Current Scientific, San Jose, California 95124, USA*

Effects of low-temperature (≈500°C) microwave annealing (MWA) of Cluster-Carbon (C_7) and Phosphorus implants are compared with rapid thermal annealing (RTA) at 900 and 1000°C for (100) and (110)-Si substrates. MWA annealing resulted in high levels of substitutional Carbon, 1.57% for (100)Si and 0.99% for (110)Si for C_7 implants. Addition of high-dose Phosphorus implants resulted in lower but still useful substitutional Carbon levels, 1.44% for (100)Si and 0.68% for (110)Si after MWA. RTA annealing at higher temperatures resulted in greatly reduced substitutional Carbon levels and deeper Phosphorus junctions. The effects of subsequent anneals by MWA and RTA methods are reported. MWA is shown to be a promising method for high-channel tensile strain in nMOSFETs with a substantially lower thermal budget than RTA.
 [DOI: 10.1149/2.010307jss]

Manuscript submitted February 28, 2013; revised manuscript received May 3, 2013. Published May 15, 2013.

Uniaxial compressive strain from Ge-rich Si:Ge (or Si_xGe_{1-x}) selective epitaxial growth in etched Si region to form source/drain contact and extensions regions has been a key process step for increasing hole mobility in pMOS channels for the last decade.[1] The corresponding approach, formation of C-rich Si:C source/drain regions as tensile stressors for nMOS channel electrons has been a much more difficult challenge. Many variations on selective Si:C epi growth in source/drain etched trenches have been explored, including epitaxial growth of the $Si_{1-x}C_x$ with the in-situ doping,[2] the selective epitaxy of an undoped $Si_{1-x}C_x$ followed by dopant implantation with dopant activation,[3] the selective epitaxy of an implanted carbon with dopant following by subsequent activation.[4] Recently selective epi Si:C source/drains have been described for 22 nm CMOS on SOI wafers.[5]

In spite of the extensive efforts and considerable progress reported on formation of selective epi Si:C stressors, implementation of the method into a production CMOS process is limited by the need for an initial deep Si etch step, difficulties in C-rich Si epi growth at high enough deposition rates to be commercially favorable and difficulties in achieving high substitutional level of C stressors and P dopants under epi growth conditions. To avoid some of these difficulties, direct implantation of C and P ions followed by recrystallization and dopant activation anneal cycles have been explored with the use of both single atom and molecular, or "cluster", ions.[4,6,7] In order to achieve high substitutional C levels, $C_{sub,eff}$, with implanted C, formation of a dense amorphous layer, formed by a pre-implant with Ge when atomic C is used or, taking advantage of the self-amorphization characteristics of molecular ions, "cluster" ion C implants, followed by solid-phase epitaxial growth during RTA or laser annealing has been reported.[6–11]

Microwave annealing, MWA, has shown the ability to re-grow amorphized damage layers and achieve high dopant activation levels while suppressing dopant diffusion for implanted dopants.[12–17] The present work investigates the use of "cluster ion" C and (single ion) P implants and MWA to achieve high $C_{sub,eff}$ and strain levels while at the same time activating P and restraining dopant diffusion. The stability of $C_{sub,eff}$ and P activation during subsequent RTA anneals is also studied.

Experimental

Samples in this work are p-type boron-doped (100) and (110) orientated Si wafers. All wafers were implanted at room temperature (RT) using a Nissin CLARIS Cluster Ion Implanter. Multiple steps of $C_7H_7^+$ implantation applied in this study were 10 keV/3 × 10^{15} cm^{-2} + 6 keV/ 8 × 10^{14} cm^{-2} + 2 keV/6 × 10^{14} cm^{-2}. The net carbon distribution was approximately a box-like profile with a peak concentration of 1 × 10^{21} cm^{-3}. Box-like profile implantation is intended to realize thicker $Si_{1-x}C_x$ films with uniform strain. In addition, selected wafers were also implanted by phosphorus (P) at 15 keV with a dose of 4 × 10^{15} cm^{-2}. Recrystallization annealing was achieved by using RTA at the temperature in the range of 900°C to 1000°C or by MWA using different microwave power magnitudes for 600 s. Microwave power was generated by magnetrons, and the power magnitude of each magnetron was around 600 W. The microwave frequency was 5.8 GHz. The microwave heating was performed in an AXOM-300 highly multi-moded chamber, manufactured by DSG Technologies. The quality of the $Si_{1-x}C_x$ film layer was investigated using several techniques. Strain and $[C]_{sub,eff}$ were derived from X-ray diffraction (XRD) rocking curves. Structural analysis was performed by cross-sectional transmission electron microscopy (TEM) images. The carbon and phosphorus profiles were measured by secondary ion mass spectrometry (SIMS) and the sheet resistances were measured with a four-point probe.

Results and Discussion

Distribution and analyze of carbon-cluster implantation.— Figure 1 shows a comparison of the temperature profiles of different dopant activation methods. The maximum temperature by MWA (provided by five magnetrons, 5P) was 540°C. The MWA process time was defined as the duration for which the microwave was turned on. In addition, anneals by RTA at 900°C for 30s and 1000°C for 10 s were used as the control splits. A N_2 flow environment was used during all annealing process. Figure 2 shows the SIMS profile of carbon concentration under different anneal conditions. The split conditions by MWA show less carbon diffusion due to its low temperature process.

Figures 3 shows TEM cross-section images the Si surface after MWA with 5 magnetrons for 600 s and RTA at 1000°C for 10 s. The Si amorphous layer created by cluster carbon implantation can be almost completely recovered by solid phase epitaxy regrowth in these anneals. However, there were some stacking faults and twins visible in the $Si_{1-x}C_x$ layer. Substitutional C levels, were calculated from analysis of the $Si_{1-x}C_x$ related peak in the XRD spectra using linear interpolations of the elastic constants and lattice parameters from reference values from Si and diamond, to yield an effective net substitutional concentration, $C_{sub,eff}$. In Fig. 4a, by MWA with higher

[z]E-mail: yjlee@ndl.narl.org.tw

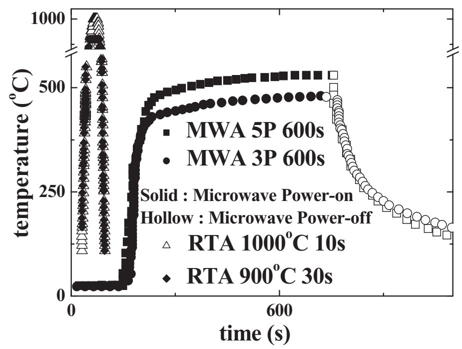

Figure 1. Comparisons of temperature profiles of different dopant activation methods. The MWA time is defined as the period when the microwave power is turned on. 5P/3P indicates microwave power was generated by five/ three magnetrons.

power (five magnetrons), the Si (100) XRD gives the highest $[C]_{sub,eff}$ (1.57%) with a maximum temperature of approximately 540°C. At lower (using 3 magnetrons) MWA power, the maximum temperature decreases from 540°C to 480°C and the $[C]_{sub,eff}$ level is reduced slightly to 1.52%. RTA anneal of Si (100) at 1000°C produced similar $[C]_{sub,eff}$ levels (1.56%)as the 5 magnetron MWA. However for RTA anneals at 900°C for 30 s, $[C]_{sub,eff}$ levels had fallen to 1.47%.

For the Si (110) samples shown in Fig. 4b, with the same annealing conditions, lower $[C]_{sub,eff}$ levels were found. The higher power MWA resulted in a $[C]_{sub,eff}$ level of 0.99% and the 3 magnetron MWA resulted in a $[C]_{sub,eff}$ level of 0.78%. The RTA anneals at either 900 or 1000°C did not result in significant $[C]_{sub,eff}$ levels in Si(110).

Phosphorus activation with the existence of carbon in the Si lattice.— In order to form effective nMOS source/drain regions using high $[C]_{sub,eff}$ levels to provide tensile stressor regions, high activation of n-type dopants is also required, with dopants, such as P, competing for substitutional sites along with C. Table I summarizes the split conditions for the study of P activation with high $[C]_{sub,eff}$ levels. In the splits of A, a, B, b, C, and c, both cluster carbon and phosphorus implants into Si substrate were both activated. The other splits, such as D, d, E, e, F, and f, the cluster carbon implants were annealed first followed by P implantation and a second anneal cycle. P was implanted at 15 keV with a dose of 4×10^{15} cm^{-2}. In some cases, effects of subsequent annealing process were investigated. The subsequent annealing methods were RTA at 1000°C for 10 s, MWA at three magnetrons for 600 s and MWA at five magnetrons for 600 s. The experimental results for $[C]_{sub,eff}$ levels and sheet resistance for the various implants, anneals and substrate orientations are collected in Table II. Figure 5 shows the relationship of Rs and $[C]_{sub,eff}$ at

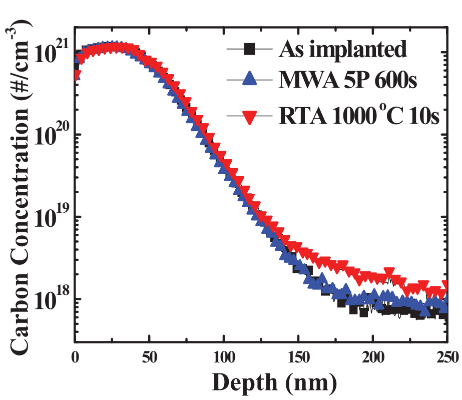

Figure 2. SIMS profiles of the carbon distribution. The $C_7H_7^+$ is implanted by 10keV at 3×10^{15} cm^{-2}, 6keV at 8×10^{14} cm^{-2} and 2keV at 6×10^{14} cm^{-2}, showing less carbon diffusion by MWA.

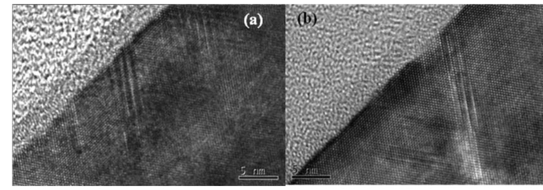

Figure 3. TEM images of $C_7H_7^+$ implanted Si (100) after (a) MWA with five magnetrons for 600s, and (b) RTA at 1000°C 10 s.

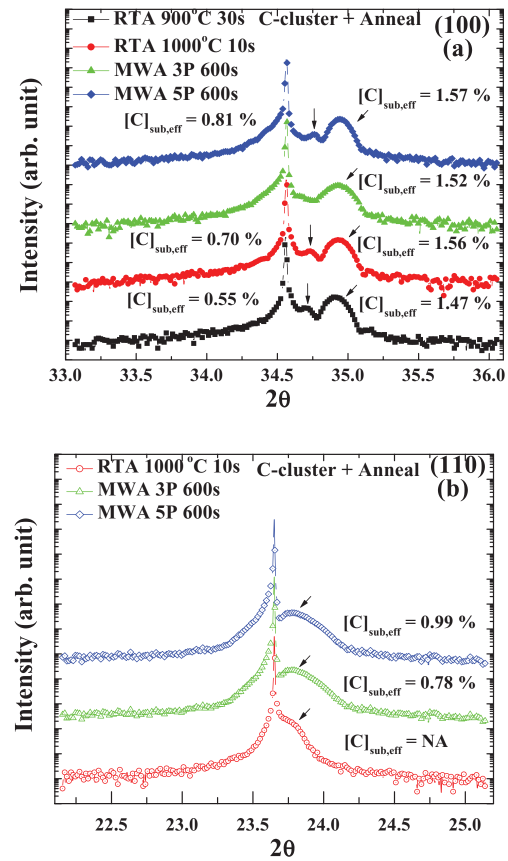

Figure 4. (a) In-plane XRD curves for $C_7H_7^+$ implanted samples with $[C]_{sub,eff}$ after different anneal conditions in (100) Si substrates. (b) in (110) Si substrates.

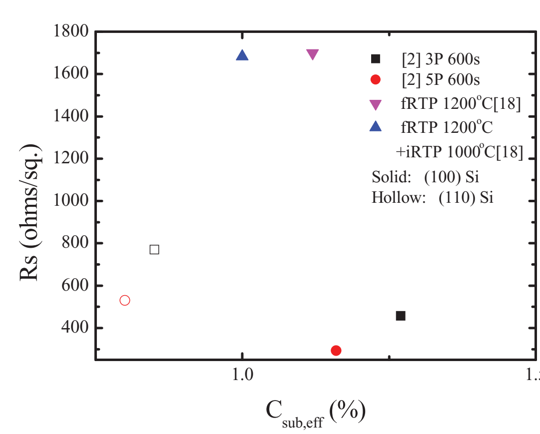

Figure 5. The relationship of Rs and $[C]_{sub,eff}$ at different MWA condition. In comparison with the results in (100) Si substrates and (110) Si substrates. The data also compare with the results of millisecond flash anneal (fRTP) and impulse spike anneal (iRTP).[18]

Table I. Split conditions for different samples.

(100)/(110)	Cluster Imp.	Anneal Condition	Dopant	Anneal Condition
A/a	C_7H_7	w/o	P	RTA 1000°C 10s
B/b	C_7H_7	w/o	P	MWA three magnetrons 600s
C/c	C_7H_7	w/o	P	MWA five magnetrons 600s
D/d	C_7H_7	RTA 1000°C 10s	P	RTA 1000°C 10s
E/e	C_7H_7	MWA three magnetrons 600s	P	MWA three magnetrons 600s
F/f	C_7H_7	MWA five magnetrons 600s	P	MWA five magnetrons 600s

1. The $C_7H_7{}^+$ is implanted by 10keV at 3×10^{15} cm^{-2}, 6keV at 8×10^{14} cm^{-2} and 2keV at 6×10^{14} cm^{-2} and the Phosphorus is implanted by 15keV at 4×10^{15} cm^{-2}.
2. w/o means without any process.

different MWA condition (3P/ 600s and 5P/ 600s). Because higher power could result in better activation, the condition of 5P/ 600s has lower sheet resistance. Then, higher power could also lead to carbon atoms to leave the substitutional sites. In comparison with the results in (100) Si substrates and (110) Si substrates, it's found higher Rs and lower $[C]_{sub.eff}$ in (110) Si substrates. It's because of more defects in (110) Si substrates. The data also compare with the results of millisecond flash anneal (fRTP) and impulse spike anneal (iRTP).[18] It's found higher $[C]_{sub.eff}$ in (100) Si substrates by using MWA.

Figures 6 shows the SIMS profiles of P, in the presence of the C profiles, for different annealing conditions. It is well known that P diffusion can be strongly reduced by co-implants with C.[19] In Figure 6 we can see that the RTA anneal at 1000°C for 10 s resulted in a clearly deeper diffused P profile than the MWA anneals, where the annealed P profiles closely follow the as-implanted case. Figure 7 shows the relationship of Rs and junction depth X_j. X_j is defined as the concentration of P is at 1×10^{19} cm^{-3}. The sheet resistance values

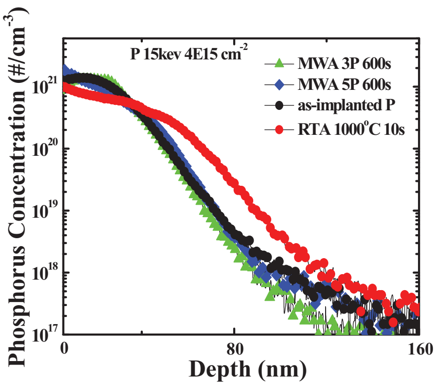

Figure 6. SIMS profile of the phosphorus distribution. The RTA 1000°C 10s shows more serious diffusion than MWA. In all MWA, the phosphorus was diffusion negligible.

Table II. Summary of $[C]_{sub}$ and sheet resistance for all implant and anneal conditions in (100) and (110) Si substrates.

Anneal Method	Anneal Conditions	$C_{sub,eff}$ (%)	Rs (ohms/sq.)	$C_{sub,eff}$ (%)	Rs (ohms/sq.)
[1] C_7 implant, Single anneal					
		(100)		(110)	
RTA	900°C 30s	1.47	na	nm	na
	1000°C 10s	1.56	na	low (<0.5)	na
MWA	3P 600s	1.52	na	0.78	na
	5P 600s	1.57	na	0.99	na
[2] C_7 + P implants, Single anneal after both implants are completed					
RTA	900°C 30s	nm	nm	nm	nm
	1000°C 10s	low	96.7	very low	134
MWA	3P 600s	1.27	457	0.85	770
	5P 600s	1.16	293	0.8	530
[3] C_7 + P implants, Anneals after each implant					
RTA	1000°C 10s	low	118	low	152
MWA	3P 600s	1.44	468	0.68	675
	5P 600s	1	300	0.63	634
[4] Extra anneal after C_7 + P implants and MWA (3P 600s)					
	none	1.27	457	0.85	770
RTA	600°C 30s	1.25	478.9	nm	nm
	750°C 30s	1.18	237.1	nm	nm
	900°C 30s	low	103.6	nm	nm
MWA	3P 600s	1.21	436.1	nm	nm
[5] Extra anneal after C_7 + MWA (3P 600s) + P + MWA (3P 600s)					
	none	1.44	468	0.68	678
RTA	600°C 30s	1.22	501.3	nm	nm
	750°C 30s	1.11	260.7	nm	nm
	900°C 30s	low	119.6	nm	nm
MWA	3P 600s	1.17	430.4	nm	nm

nm = not measure.
na = not applicable.
"low" means the $Si_{1-X}C_X$ related peak is not distinct.

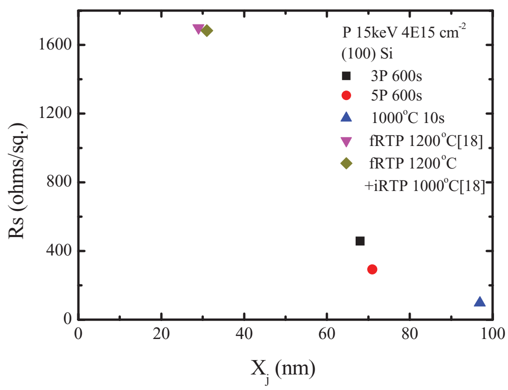

Figure 7. Rs versus SIMS-X_j for various annealing condition, where X_j is called junction depth. X_j is defined as the concentration of P is at 1×10^{19} cm^{-3}.

for C_7 and P co-implants were substantially lower following the RTA 1000 C/ 10 s anneal (96.7 Ohms/sq.) compared to MWA process (457 Ohms/sq. for the 3P/ 600s and 293 Ohms/sq. for the 5P/ 600s anneal), as one could expect from the deeper junction depth for the RTA process. From the results of fRTP and fRTP + iRTP, shallower X_j leaded to higher Rs. However, lower $[C]_{sub.eff}$ in (100) Si substrates is unfavorable.

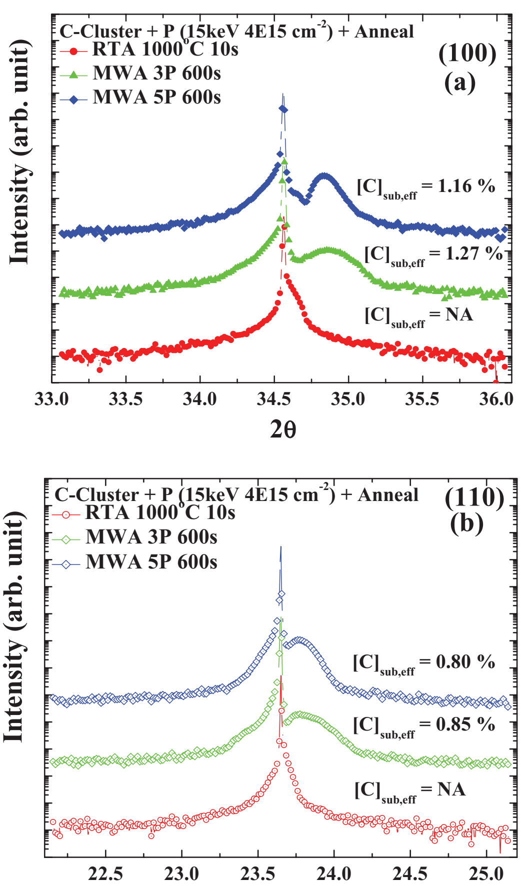

Figure 8. (a) In-plane XRD curves for $C_7H_7^+$ implanted and phosphorus samples with $[C]_{sub,eff}$ after the all anneal conditions: RTA 1000°C for 10 s, MWA three and five magnetrons anneal for 600s at orientation (100) substrate. (b) the same conditions with (110) substrate.

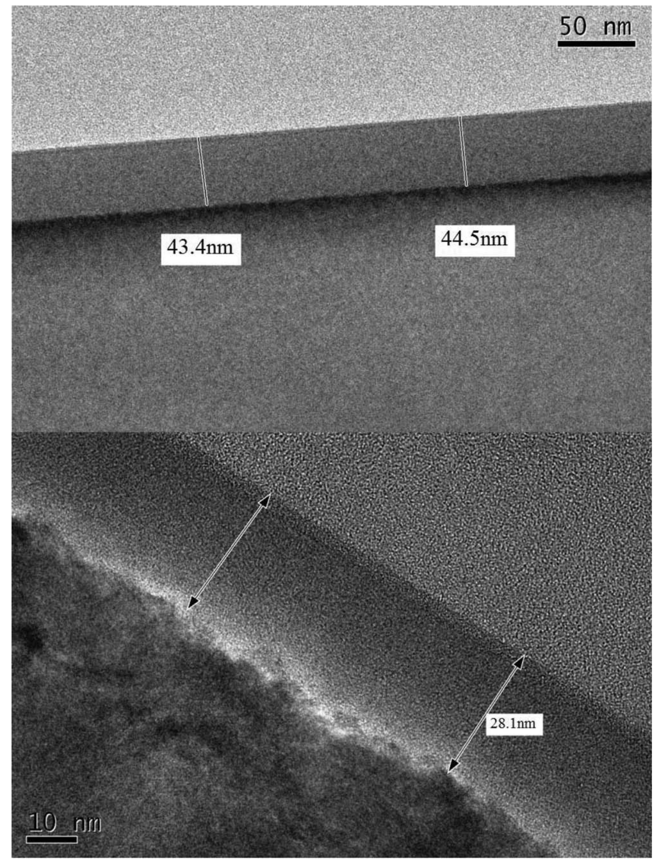

Figure 9. TEM images of (100) Si with carbon-cluster and phosphorus doping after (a) as-implented, (b) MWA three magnetrons 600s.

Figure 8 shows the XRD spectra and the $[C]_{sub,eff}$ levels for the splits A/a, B/b and C/c, with only a single anneal cycle for the C_7 and P implants, in Si (100) and (110) substrates. In Fig. 8a, for the Si (100) substrates, a higher $[C]_{sub,eff}$ level (1.16%) was obtained by MWA than by RTA 1000°C anneal, where no substantial $[C]_{sub,eff}$ levels were seen. These $[C]_{sub,eff}$ levels for the C_7 and P co-implants were lower than the results for similar anneals with the C_7 implants alone, reflecting the competition between C and P for substitutional sites for strain effect and electrical activation. Co-implants of C_7 and P into Si(110) substrates resulted in significantly lower $[C]_{sub,eff}$ levels, shown in Fig. 8b, and higher sheet resistances than corresponding annealing conditions into Si(100).

Additional annealing steps following the C_7 implants, splits D/d, E/e and F/f, resulted in modest and mixed changes in $[C]_{sub,eff}$ levels and sheet resistance values compared to the single anneal cases. In most of the cases tested, the addition of the second anneal cycle actually increased the sheet resistance values for both RTA and MWA anneals. In the case of the 3P/ 600 s MWA, the use of an anneal cycle after each of the C_7 and P implants resulted in a $[C]_{sub,eff}$ level nearly equal to (1.44%) the levels for the C_7 implants alone (1.47 to 1.57 depending on the anneal used).

Metastability of $[C]_{sub,eff}$ by post annealing process.— The metastable nature of $C_{sub,eff}$ levels with additional anneal process for the P-doped $Si_{1-x}C_x$ film was investigated in Si(100) substrates with a series of extra RTA or MWA cycles following C_7 and P co-implants with either single or double MWA at 3P/ 600 s. The extra anneal conditions and experimental results are listed in the lower two sections of Table II. Prior to the "extra" anneals, the MWA with 3P/ 600s conditions for C_7 and P co-implants resulted in only partial regrowth of the as-implanted 44 nm thick amorphous layer, as shown

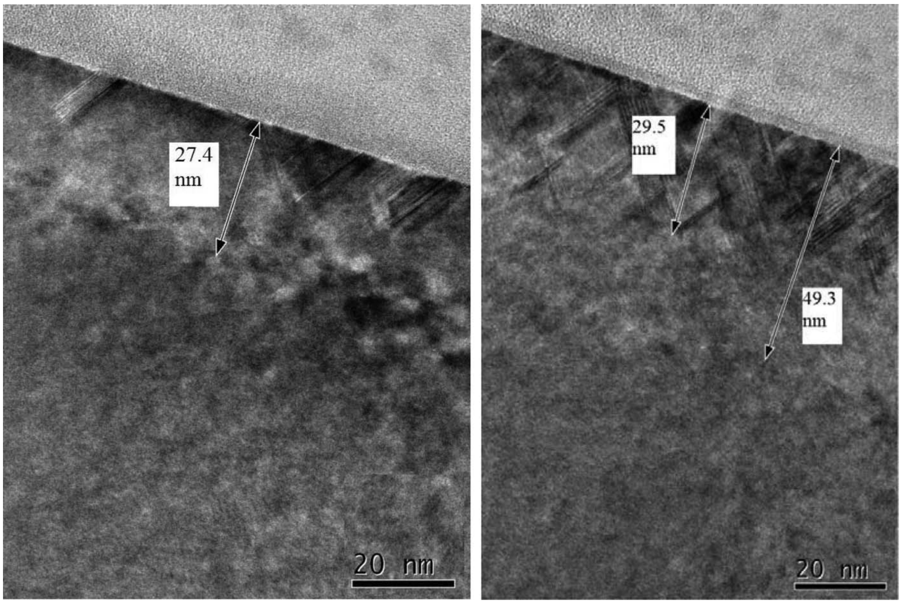

Figure 10. TEM images of (100) Si with carbon-cluster and phosphorus doping after (a) MWA three magnetrons 600s twice and (b) MWA three magnetrons 600 s + RTA 750°C 30 s.

in the TEM images in Fig. 9. Note that the higher power MWA at 5P/600 s resulted in complete amorphous layer re-growth, see Fig. 3. As shown in the TEM images in Fig. 10, the addition of an extra anneal of either another MWA at 3P/ 600 s or an RTA at 750°C / 30 s was enough to complete the re-growth of the implant generated amorphous layer. However, the surface regions, starting near the depth at 28 nm of the residual amorphous layer after the initial MWA at 3P/ 600s, showed a high density of twin-like defects, with a higher defect density for the RTA extra anneal. Similar twin-like defects have been found in other C-rich Si layers, such those found in undoped Si:C layers grown by CVD methods at 550°C with $[C]_{sub,eff}$ levels (0.6 to 1.5%) similar to those in this study.[20] The CVD growth study reported $[C]_{sub,eff}$ levels that saturated at 1.2% for 30 nm thick Si:C layers, rising to 1.6% for 10 nm layers. In contrast, the implant and MWA anneal results reported here are in much thicker (≈100 nm) C-rich layers and $[C]_{sub,eff}$ levels at ≈1.5%, all with the high active dopant levels of P required to form useful source/drain junctions.

All of the "extra" anneals resulted in decreases in $[C]_{sub,eff}$ levels. In the case of the RTA cycles, 30 s anneals at 750°C and above strongly reduced $[C]_{sub,eff}$ levels, with anneals at 900°C resulting in extinction of measurable C-based strain effects. The addition of a single MWA at 3P/ 600s after an initial process also results in modest but measurable reductions in $[C]_{sub,eff}$ levels. All of these results highlight the meta-stable nature of $[C]_{sub,eff}$ levels in the range of 1 to 2% to exposure to additional thermal cycles. Extra RTA anneals at 750 and 900°C resulted in strongly reduced sheet resistance, as expected from the deeper junctions formed with additional P diffusion. The extra MWA step with 3P conditions resulted in only modest sheet resistance reductions.

Conclusions

In this study, the substitutional carbon concentration ($[C]_{sub,eff}$) of 1.57% and 0.99% in (100) and (110) Si substrates could be reached by MWA. The lower temperature MWA could achieve higher $[C]_{sub,eff}$ levels than the RTA process. In addition, MWA process could also suppress the dopant diffusion, including P and maintain high $[C]_{sub,eff}$ levels with C_7 and P co-implants needed to form source/drain regions with high tensile strains on nMOS channel regions. The lower thermal budgets for MWA, with maximum temperatures used here at ≈500°C, provide a valuable range of process options for advanced transistor fabrication.

Acknowledgment

This work is supported in part by the National Science Council (NSC), Taiwan under Contract NSC-97-1221-E-009-152-MY3, NSC-98-2221-E-492-019, NSC-98-2221-E-212-033-MY3.

References

1. P. Packan, S. Cea, H. Despande, T. Ghani, M. Giles, O. Golonzka, M. Hattendorf, R. Kotlyar, K. Kuhn, A. Murthy, P. Ranade, L. Shifren, C. Weber, and K. Zawadzki, IEDM08., (2008).
2. B. Yang, R. Takalkar, Z. Ren, L. Black, A. Dube, J. W. Wejtmans, J. Li, J. B. Johnson, J. Faltermeier, A. Madan, Z. Zhu, A. Turanski, G. Xia, A. Chakravarti, R. Pal, K. Chan, A. Reznicek, T. N. Adam, J. P. de Souza, E. C. T. Harley, B. Greene, A. Gehring, M. Cai, D. Aime, S. Sun, H. Meer, J. Holt, D. Theodore, S. Zollner, P. Grudowski, D. Sadana, D.-G. Park, D. Mocuta, D. Schepis, E. Maciejewski, S. Luning, J. Pellerin, and E. Leobandung, *IEDM Tech.* 51 (2008).
3. K. W. Ang, K. J. Chui, V. Bliznetsov, Y. Wang, L.-Y. Wong, C.-H. Tung, N. Balasubramanian, M.-F. Li, G. Samurda, and Y.-C. Yeo, *IEDMTech.*, 497 (2005).
4. Y. Liu, O. Gluschenkov, J. Li, A. Madan, A. Oszan, B. Kim, T. Dyer, A. Chakravarti, K. Chan, C. Lavoie, I. Popova, T. Pinto, N. Rovedo, Z. Luo, R. Loesing, W. Henson, and K. Rim, *VLSI Tech.*, 44 (2007).
5. S. Narasimha, P. Chang, C. Ortolland, D. Fried, E. Engbrecht, K. Nummy, P. Parries, T. Ando, M. Aquilino, N. Arnold, R. Bolam, J. Cai, M. Chudzik, B. Ciriany, G. Costrini, M. Dai, J. Dechene, C. DeWan, B. Engel, M. Gribelyuk, D. Guo, G. Han, N. Habib, J. Holt, D. Ioannou, B. Jagannathan, D. Jaeger, J. Johnson, W. Kong, J. Koshy, R. Krishnan, A. Kumar, M. Kumar, J. Lee, X. Li, C.-H. Lin, B. Linder, S. Lucarini, N. Lustig, P. McLaughlin, K. Onishi, V. Ontalus, R. Robison, C. Sheraw, M. Stoker, A. Thomas, G. Wang, R. Wise, L. Zhuang, G. Freeman, J. Gill, E. Maciejewski, R. Malik, J. Norum, and P. Agnello, IEDM12, (2012).
6. A. Li-Fatou, A. Jain, W. Krull, M. Ameen, M. Harris, and D. Jacobson, *ECS Trans.*, **11**(6), 125 (2007).
7. K. Sekar, N. Tokoro, H. Onoda, Y. Nakashima, Y. Koga, N. Hamamoto, T. Nagayama, J. Herman, S. Novak, M. Rodgers, D. Franca, and S. Vivekanand, *International Workshop on Junction Technology*, IWJT12 (2012).
8. H. Itokawa, K. Miyano, Y. Oshima, I. Mizushima, and K. Suguro, *Jpn. J. Appl. Phys.*, **49**, 04DA05 (2010).
9. A. Tian-Yi Koh, R. Tek-Po Lee, Fang-Yue Liu, Tsung-Yang Liow, Kian Ming Tan, Xincai Wang, Ganesh S. Samudra, N. Balasubramanian, Dong-Zhi Chi, and Yee-Chia Yeo, *IEEE Electron Device Lett.*, **29**, 464 (2008).
10. Yee-Chia Yeo, *Semicond. Sci. Technol.*, **22**, s177 (2007).
11. Shao-Ming Koh, Karuppanan Sekar, David Lee, Wade Krull, Xincai Wang, Ganesh S. Samudra, and Yee-Chia Yeo, *IEEE Electron Device Lett.*, **29**, 1315 (2008).
12. T. L. Alford, D. C. Thompson, J. W. Mayer, and N. David Theodore, *J. Appl. Phys.*, **106**, 114902 (2009).
13. Y. J. Lee, Y. L. Lu, F. K. Hsueh, K. C. Huang, C. C. Wan, T. Y. Cheng, M. H. Han, J. M. Kowalski, J. E. Kowalski, D. Heh, H. T. Chuang, Y. Li, T. S. Chao, C. Y. Wu, and F. L. Yang, *IEDM Tech.*, 31 (2009).

14. Y. L. Lu, F. K. Hsueh, K. C. Huang, T. Y. Cheng, J. M. Kowalski, J. E. Kowalski, Y. J. Lee, T. S. Chao, and C. Y. Wu, *IEEE Electron Device Lett.*, **31**, 437 (2010).
15. H. Bosman, W. Tang, Y. Y. Lau, and R. M. Gilgenbach, *Appl. Phys. Lett.*, **85**, 3319 (2004).
16. K. Thompson, Y. B. Gianchandani, J. Booske, and R. F. Cooper, *J. Microelectromech. Syst.*, **11**, 285 (2002).
17. K. Thompson, J. H. Booske, Y. B. Gianchandani, and R. F. Cooper, *IEEE Electron Device Lett.*, **23**, 127 (2002).
18. K. Sekar, W. Krull, J. Chan, S. McCoy, and J. Gelpey, *16th IEEE International Conference on Advanced Thennal Processing of Semiconductors - RTP2008*, 107 (2008).
19. S. B. Felch, E. Collart, V. Parihar, S. Thirupapuliyur, R. Schreutelkamp, B. J. Pawlak, T. Hoffmann, S. Severi, P. Eyben, W. Vandervorst, and T. Noda, *J. Vac. Sci. Technol. B*, **26**, 281 (2008).
20. N. Cherkashin, M. J. Hytch, F. Houdelier, F. Hue, V. Paillard, A. Claverie, A. Gouye, O. Kermarrec, D. Rouchon, M. Burdin, and P. Holliger, *Appl. Phys. Lett.*, **94**, 141910 (2009).